Journal of Chromatography A, 1274 (2013) 44–53

Contents lists available at SciVerse ScienceDirect

Journal of Chromatography A

journal homepage: www.elsevier.com/locate/chroma

Development of novel molecularly imprinted magnetic solid-phase extraction materials based on magnetic carbon nanotubes and their application for the determination of gatifloxacin in serum samples coupled with high performance liquid chromatography

Deli Xiao[a], Pierre Dramou[a], Nanqian Xiong[b], Hua He[a,c,*], Hui Li[a], Danhua Yuan[a], Hao Dai[a]

[a] Department of Analytical Chemistry, China Pharmaceutical University, Nanjing 210009, China
[b] School of Chemistry and Life Science, Guizhou Normal College, Guizhou 550003, China
[c] Key Laboratory of Drug Quality Control and Pharmacovigilance, Ministry of Education, China Pharmaceutical University, Nanjing 210009, China

ARTICLE INFO

Article history:
Received 9 September 2012
Received in revised form
29 November 2012
Accepted 5 December 2012
Available online 13 December 2012

Keywords:
Molecularly imprinted polymers
Magnetic carbon nanotubes
Magnetic solid phase extraction
Gatifloxacin
Serum samples

ABSTRACT

A novel composite imprinted material, on the basis of magnetic carbon nanotubes (MCNTs)-incorporated layer using gatifloxacin as a template, methacrylic acid as a functional monomer, and ethylene glycol dimethacrylate as a cross-linker, was successfully synthesized by a surface imprinting technique. Adsorption dynamics and a Scatchard adsorption model were employed to evaluate the adsorption process. The results showed that magnetic carbon nanotubes molecularly imprinted polymers (MCNTs@MIP) displayed a rapid dynamic adsorption and a high adsorption capacity of 192.7 μg/mg toward GTFX. Applied MCNTs@MIP as a sorbent, a magnetic solid phase extraction method coupled with high performance liquid chromatography (MSPE-HPLC) was developed for the determination of GTFX in serum samples. The recoveries from 79.1 ± 4.8% to 85.3 ± 4.2% were obtained. MCNTs@MIP can not only be collected and separated fast by external magnetic field but also have high surface-to-volume ratio, outstanding mechanical properties and specific recognition toward template molecule. In addition, the MCNTs@MIP could be regenerated, which could be used for five cycles with lost of less than 7.8% of its recovery on average. These analytical results of serum samples display that the proposed method based on MCNTs@MIP is applicable for fast and selective extraction of therapeutic agents from biological fluids.

1. Introduction

The fluoroquinolones, which comprise a relatively large and constantly expanding group of substances, have emerged as one of the most important class of antibiotics [1]. Gatifloxacin (GTFX), (±)-1-cyclopropyl-6-fluoro-1,4-dihydro-8-methoxy-7-(3-methyl-1-piperazinyl)-4-oxo-3-quinoline carboxylic acid (Fig. S1), is an effective antibiotic of the fourth generation fluoroquinolone family with expanded activity against gram-positive bacteria and atypical pathogens by inhibiting the bacterial enzymes DNA gyrase and topoisomerase IV [2]. Although GTFX has been widely used as an effective antibiotic, its bioavailability is relatively low when used in some special physiological environments such as trans-corneal, trans-dermal and trans-lymphatic systems which need a long residence time and prolonged high drug concentration, a large amount of GTFX eventually enters into blood through the mucosa absorption, which may cause side effects like dyspnea, arrhythmia and pathoglycemia [3], therefore, the determination procedure of GTFX in biological samples is important for protecting human health.

Several methods have been described for the determination of GTFX in biological samples, including spectrophotometry [4], spectrofluorimetry [5], polarography [6], voltammetry [7], chemiluminescence [8] and high performance liquid chromatography (HPLC) [1,9–12]. The method based on HPLC is the universal method of the quantitative determination of GTFX. However, these methods are unsatisfactory because of the extremely low GTFX concentration and interference of complex matrix in serum sample, several isolation and enrichment processes were required and the analytical procedure was always time-consuming and solvent-depending [5,11]. Thus, to utilize a solid adsorbent with specific recognition and time-saving property for serum sample preparation would be a feasible way to solve those aforementioned problems.

Owing to the chemical, mechanical and thermal stability together with high selectivity for template molecules, molecularly imprinted polymers (MIPs) have been utilized for a wide variety

* Corresponding author at: China Pharmaceutical University, 24 Tongjia Lane, Nanjing 210009, Jiangsu Province, China. Tel.: +86 025 83271505; fax: +86 025 83271505.
E-mail addresses: dochehua@163.com, jcb315@163.com (H. He).

0021-9673/$ – see front matter © 2012 Elsevier B.V. All rights reserved.
http://dx.doi.org/10.1016/j.chroma.2012.12.011

of applications, including chromatography [13], protein separation [14], solid-phase extraction [15], drug-controlled release [2,16] and sensor devices [17,18]. The imprinting technique is a well-established and simple technique for synthesizing materials with specific molecular recognition properties [19–21]. Although the bulk MIP prepared by conventional methods exhibits high selectivity [22,23], some disadvantages were suffered, such as the heterogeneous distribution of the binding sites, embedding of most binding sites, and poor site accessibility for template molecule [24]. To resolve these problems, scientists have made efforts to prepare core–shell structural MIP. By preparing the MIP film on a solid–support substrate, the surface-imprinting technique provides an alternative way to improve mass transfer and reduce permanent entrapment of the template. In previous investigations, SiO_2 [25,26], TiO_2 [27] and Fe_3O_4 [28–31] have been widely used in the surface-imprinting process.

Recently, in order to avoid leakages and fragility of traditional support materials, special attentions have been directed to combine magnetic nanoparticles (MNPs) with nanosized materials such as carbon nanotubes (CNTs) for magnetic carbon nanotubes (MCNTs) preparation. Various MCNT synthetic methods have been described in the literatures. Correa-Duarte et al. have synthesized MCNTs through a layer-by-layer assembly approach [32]. Georgakilas et al. have used pyrene as interlinker for the attachment of capped magnetic nanoparticles on the surface of CNTs [32,33]. Gao et al. have prepared MCNTs via the electrostatic attraction between CNTs and magnetic nanoparticles [34]. Jia et al. have combined magnetite beads with CNTs based on a hydrothermal technique [35]. We prepared MCNTs by a simple solvothermal process, which can easily alter the size (100–350 nm), location and denseness of Fe_3O_4 beads fixed on CNTs as well as the MCNT structure via controlling the reaction parameters [36].

To the best of our knowledge, although some researches studied MIP using fluoroquinolone as template [37–39], there is no report of the preparation of molecularly imprinted polymers on the surface of magnetic carbon nanotubes (MCNTs@MIP) and application for magnetic solid phase extraction. When MCNTs are encapsulated inside of MIP, the resulting MCNTs@MIP can be easily collected and separated by an external magnetic field without additional centrifugation or filtration [40,41], which makes separation easier and faster. Besides, MCNTs@MIP could have outstanding mechanical properties of CNTs. Moreover, MCNTs@MIP can not only selectively recognize the template molecules in complex matrix but also possess more imprinted cavities within the polymer network due to the high surface-to-volume ratio of MCNTs [42]. Therefore, this work focused on a simple and effective method to synthesize novel MIP based on magnetic carbon nanotubes and the application in magnetic solid phase extraction. The adsorption kinetics, static adsorption and selective recognition of MCNTs@MIP were investigated in detail. And then MCNTs@MIP were used in magnetic solid phase extraction of GTFX in serum samples.

2. Experimental

2.1. Materials

Ferric chloride hexahydrate ($FeCl_3{\cdot}6H_2O$), sodium acrylate ($CH_2{=}CHCOONa$, Na acrylate), sodium acetate (CH_3COONa, NaOAc), ethylene glycol (EG), diethylene glycol (DEG), methacrylic acid (MAA), ethylene glycol dimethacrylate (EGDMA), polyvinylpyrrolidone (PVP) and azobisisbutyronitrile (AIBN) were obtained from Aladdin. Gatifloxacin (GTFX) and pazufloxacin (PZFX) were purchased from Sinopharm Chemical Reagent Co. Ltd., China. Carbon nanotubes with outer diameter 10–20 nm and length 5–15 μm were purchased from Shenzhen Nanotechnologies Port Co. Ltd., China.

2.2. Instruments and HPLC analysis

UV–vis absorption was characterized by UV1800 UV-Vis spectrophotometer (Shimadzu Corporation, Japan). The morphology of the as-synthesized nanoparticles was studied using a S-3000 scanning electron microscopy (SEM, Hitachi Corporation, Japan) and a FEI Tecnai G2 F20 transmission electron microscope (TEM). The surface groups on the as-synthesized nanoparticles were measured with a 8400 s FT-IR spectrometer (Shimadzu Corporation, Japan). Phase identification was done by the X-ray powder diffraction (XRD) pattern, using X' TRA X-ray diffractometer with Cu Kα irradiation at $\gamma = 0.1541$ nm.

The HPLC analyses were performed on a Shimadzu LC-20AT HPLC system including a binary pump and a diode array detector (Shimadzu, Kyoto, Japan). A Shimadzu VP-ODS C18 (5 μm particle size, 250 mm × 4.6 mm) analytical column was used for analyte separation. The mobile phase was a mixture of triethylamine phosphate (1%, pH 4.30)–acetonitrile (13/87, v/v) delivered at a flow rate of 1.0 mL/min. The injection volume was 20 μL, and the column effluent was monitored at 325 nm.

2.3. Synthesis of MCNTs

As shown in Fig. 1, carboxylation of CNTs (c-CNTs) was carried out by blending the CNTs (0.5 g) with 100 mL of sulfuric acid and nitric acid mixture (mole ratio: 3/1). This solution was dispersed by ultrasonication for about 2 h and refluxed under magnetic stirring at 80 °C for 12 h. Then, the dispersed solution was filtered and the particles obtained were washed to neutrality, and dried in vacuum at 65 °C overnight.

The preparation of MCNTs was carried out according to our previous work [36]. c-CNTs (0.4 g), $FeCl_3{\cdot}6H_2O$ (2.4 g, 9 mmol), Na acrylate (3.4 g) and NaOAc (3.4 g) were added into a mixture of ethylene glycol (EG, 22.5 mL) and diethylene glycol (DEG, 22.5 mL) under ultrasonication for about 1 h. The homogenous black solution obtained was transferred to a Teflon-lined stainless-steel autoclave and sealed to heat at 200 °C. After reaction for 10 h, the autoclave was cooled to room temperature. The MCNTs obtained were washed several times with ethanol and water, and then dried in vacuum at 65 °C for 10 h. In parallel, a reference was prepared by the same protocol with magnetic nanoparticles (MNPs), but without adding c-CNTs.

2.4. Synthesis of MCNTs@MIP

In a typical procedure, MCNTs@MIP were synthesized as follows: the GTFX (1.0 mmol) was dissolved in 10 mL of DMSO, and then 4.0 mmol of MAA was added into it. This mixture was stirred for 30 min for preparation of the preassembly solution. The MCNTs (1.0 g) were mixed with 4 mL of dimethylsulfoxide (DMSO) and ultrasounded for 5 min. Then 20 mmol of EGDMA and the preassembly solution were added into the mixture of MCNTs in DMSO. This mixture was subjected to ultrasound for 30 min for the preparation of the prepolymerization solution. The PVP (0.4 g) used as dispersant was dissolved into 100 mL of DMSO:water (9:1, v/v) in a three-necked round-bottomed flask. The mixture was stirred at 300 rpm and purged with nitrogen gas to displace oxygen while the temperature increased to 60 °C. The prepolymerization solution was added into the three-necked flask, and then 0.1 g of AIBN was also added into it. The reaction was allowed to proceed at 60 °C for 12 h. After the polymerization, the polymers were separated and washed with methanol:acetic acid (6:4, v/v) several times under ultrasound until the template molecule could not be detected by

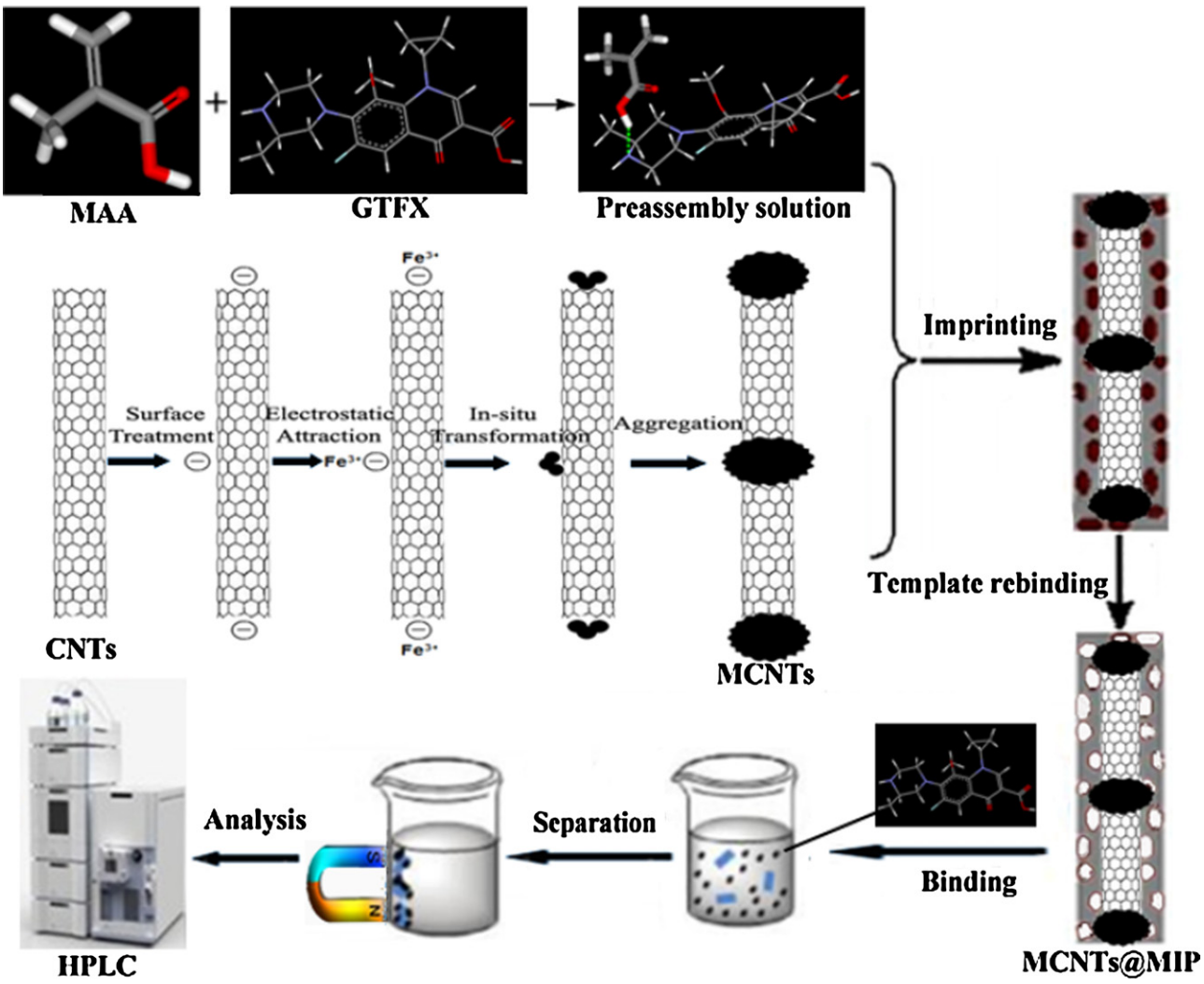

Fig. 1. Scheme of the synthetic route for MCNTs@MIP and their application for SPE of GTFX with the help of an applied magnetic field.

HPLC. The polymers were washed with water three times again and dried at 60 °C.

The molecularly nonimprinted polymers on the surface of magnetic carbon nanotubes (MCNTs@NIP) were prepared and processed similarly as above, except that the template molecule GTFX was not added.

Moreover, the molecularly imprinted polymers and molecularly nonimprinted polymers based on magnetic nanoparticles (MNPs@MIP and MNPs@NIP, respectively) were also prepared by a similar way.

2.5. Binding experiments

In kinetic adsorption experiments, 50 mg of MCNTs@MIP and MNPs@MIP were mixed with 50 mL of GTFX at a concentration of 400 μg/mL, respectively, and incubated at regular time intervals, and then the supernatants and polymers were separated by a permanent magnet. The GTFX concentration of the supernatants was measured by HPLC analysis. According to variance of GTFX concentration before and after adsorption, the equilibrium adsorption capacity (Q, μg/mg) of GTFX bound to the imprinted polymers is calculated by Eq. (1).

$$Q = (C_0 - C_1) \cdot \frac{V}{m} \quad (1)$$

where C_0 and C_1 represent the initial solution concentration and the final solution concentration (μg/mL) of GTFX, respectively. V represents the volume of the solution (mL) and m represents the weight of the polymer (mg). The average data of triplicate independent results were used for the following discussion.

Static equilibrium adsorption experiments were conducted by using screw-capped glass centrifuge tubes as batch reactor systems. Each tube containing 20 mg MCNTs@MIP, MCNTs@NIP, MNPs@MIP and MNPs@NIP respectively was filled with 2 mL GTFX solution at different concentrations. All tubes were immediately sealed and shaken with a rotary shaker at 150 rpm for 1 h. The amount of GTFX bound to the MCNTs@MIP, MCNTs@NIP, MNPs@MIP and MNPs@NIP was determined by HPLC.

2.6. Adsorption selectivity

A mixture standard solution of GTFX, CPFX, PZFX and AMX with initial concentration of 400 μg/mL was incubated with MCNTs@MIP, MCNTs@NIP, MNPs@MIP and MNPs@NIP, and the extraction procedure was then conducted as described earlier in static equilibrium adsorption experiments.

2.7. Determination of GTFX in serum samples

The blank human serum samples were obtained by centrifugation at 3500 rpm for 10 min and the supernatants were stored

at −20 °C until used. A simple and effective SPE procedure was adopted for this study. A 2.5 mL aliquot of blank serum spiked with 2.5 mL of gatifloxacin and pazufloxacin standard solution at a concentration of 400 μg/mL was loaded onto 50 mg MCNTs@MIP and MNPs@MIP, respectively. After incubation for 1 h at room temperature, MCNTs@MIP and MNPs@MIP were removed by a permanent magnet and washed with 5 mL of water. Then 5 mL mixture of methanol/acetic acid (6:4, v/v) was used to elute GTFX. The elute solution was concentrated with nitrogen gas and then quantified to the volume of 0.5 mL with triethylamine phosphate/acetonitrile (13/87, v/v). At last, the treated samples were submitted to HPLC for quantitative analysis.

3. Results and discussion

3.1. Synthesis of MCNTs@MIP

Fig. 1 illustrates the proposed overall synthetic procedure of MCNTs@MIP and their application for MSPE of GTFX. The synthetic approach included the following procedure: (1) obtaining MCNT cores; (2) self-assembly of the template and functional monomers; (3) polymerization of the polymeric mixture in the presence of crosslinker, initiator and dispersing medium and (4) achieving recognition cavities of the resulting beads by eluting template molecules.

MCNTs can be one of the most promising supports of MIP because the resulting MCNTs@MIP retain the affinity and selectivity toward template molecule, while adding several benefits including high mechanical strength, large specific surface area and high saturation magnetization. Initially, treating CNTs with concentrated H_2SO_4/HNO_3 mixture is a classic method of creating a large amount of negatively charged functional groups such as carboxyl on the surface of CNTs. In the solvothermal process, positive metal ions (ferric ions) in the system and the carboxylic groups would interact through electrostatic attraction, and the positive metal ions can be served as nucleation precursors. The reduction reaction can turn some of these ferric ions into ferrous ions and then they can coprecipitate into Fe_3O_4 crystallites on the surface of CNTs to form Fe_3O_4/CNTs composites. Herein, NaOAc, Na acrylate, EG and DEG play important roles in the formation of MCNTs. It has been reported that Fe^{3+} cannot be reduced by EG alone [43]. Therefore, NaOAc was used to assist the EG/DEG in reducing $FeCl_3$ into Fe_3O_4 by modifying the alkalinity of the system. The hydrolysis rate of $FeCl_3$ could be accelerated by increasing alkalinity to promote the formation of larger Fe_3O_4 nanocrystals [44]. Sodium acrylate was coated with the formed Fe_3O_4 nanograins due to the strong coordination between ferric ions and carboxylate. The formed polyacrylate in situ would stabilize the primary Fe_3O_4 nanograins, and confine them to form larger Fe_3O_4 grains in the recrystallization process [45]. EG plays both roles as a reducing agent and as a solvent during the formation of the Fe_3O_4 particles [46].

In order to acquire high adsorption capacity, the synthesis conditions of MCNTs@MIP, including the molar ratios of template molecule to functional monomer to cross-linker (T:M:C), and polymerization temperature and time, were optimized. As shown in Table S1, the molar ratios among template molecule, functional monomer and cross-linker affected greatly the adsorption capacity due to the changes of the quality of MIP and the number of recognition sites in the MIP. High ratios of the functional monomer to the template result in high nonspecific affinity, while low ratios lead to fewer template and functional monomer complexes due to an insufficient number of functional groups [47]. Adsorption capacity increases with the amount of functional monomer and crosslinker, due to the augment in the number of recognition cavities in the MCNTs@MIP. However, MCNTs@MIP agglomeration occurs when excessive amounts of monomer and crosslinker are used at the preparation stage [48]. The results revealed that the optimum molar ratio of template molecule to functional monomer to crosslinker was 1:4:20 (No. 3), so that ratio was used in the remainder of this work.

Polymerization temperature and time played important roles in the shape and size distribution of composites [49]. Long polymerization time (18 h, No. 11) or high temperature (80 °C, No. 9) would increase surface thickness and particle size of MCNTs@MIP, resulting in low adsorption capacity. As polymerization time decreased to 12 h and temperature decreased to 60 °C (No. 3), the resulting MCNTs@MIP showed the highest adsorption capacity due to the well three-dimensional imprinted cavities coated on the surface of MCNTs. However, further decreasing the polymerization temperature (40 °C, No. 8) or shortening the polymerization time (6 h, No. 10) led to lower adsorption capacity, which could be attributed to less imprinting recognition sites for the GTFX. After optimizing the ratios of T:M:C, polymerization temperature and time, this method for synthesizing imprinted stationary phase could also be applied to other organic template molecules.

3.2. Characterization

Fig. S2 represents the XRD pattern of the MNPs and MCNTs. Compared with MNPs, the XRD pattern of MCNTs had the diffraction peaks of cubic Fe_3O_4, which can be readily indexed according to JCPDS file no. 75-0033, and the diffraction peak at $2\theta = 26°$, which can be indexed to (0 0 2) reflection of the c-CNTs [35]. No obvious peaks from other phases are observed, indicating that the product obtained was a mixture of two phases: cubic Fe_3O_4 and c-CNTs. The main peaks of Fe_3O_4 in the XRD pattern are broadened, indicating the crystalline portion of the Fe_3O_4 particle is very small and the Fe_3O_4/CNTs composites are applicable as supports of nanosized MIP.

The morphologies of MNPs, MNPs@MIP, MCNTs and MCNTs@MIP were obtained by TEM (Fig. 2). As shown in Fig. 2C, the diameter of the wall and length of CNTs were about 20–30 nm and several micrometers, respectively. Fe_3O_4 nanoparticles with diameters of 100–200 nm were deposited onto the surfaces of the CNTs. Fig. 2B and D shows the formation of MNPs@MIP and MCNTs@MIP core@shell structured nanocomposites after the template–monomer complex was reacted on the surface of MNPs and MCNTs, respectively. Compared with MNPs and MCNTs, the diameter of MNPs@MIP and MCNTs@MIP was increased after being coated with a layer of MIP with an average thickness of 30–40 nm.

The magnetism of c-CNTs, MNPs@MIP and MCNTs@MIP is displayed in Fig. 3. It was observed that MNPs@MIP and MCNTs@MIP could be easily separated from the aqueous solution within few seconds by placing a permanent magnet near the glass bottle and the supernatant was colorless (Fig. 3B and C).

Fig. 4 shows the surface groups on c-CNTs, MNPs, MCNTs, MNPs@MIP and MCNTs@MIP analyzed by FT-IR. Several significant bands in Fig. 4A are attributed to carboxylic acid groups introduced by acid oxidizing, including the appearance of C=O stretching band at 1735 cm^{-1}, COO^- asymmetric stretching band at 1620 cm^{-1} and O—H stretching band at 3421 cm^{-1}. While the Fe—O characteristic band at 583 cm^{-1} is indicative of Fe_3O_4 in Fig. 4B. The FT-IR spectra of MCNTs composites (Fig. 4C) shows at 1735 cm^{-1} for C=O stretching band, 1620 cm^{-1} for COO^- asymmetric stretching band, 3421 cm^{-1} for O—H stretching band and 583 cm^{-1} for Fe—O characteristic band, indicating that MCNTs are composed of c-CNTs and MNP. Comparing with Fig. 4B and C, the increase of C—H asymmetric stretching band at 2970 cm^{-1}, C=O stretching band at 1735 cm^{-1} and COO^- asymmetric stretching band at 1620 cm^{-1} in Fig. 4D

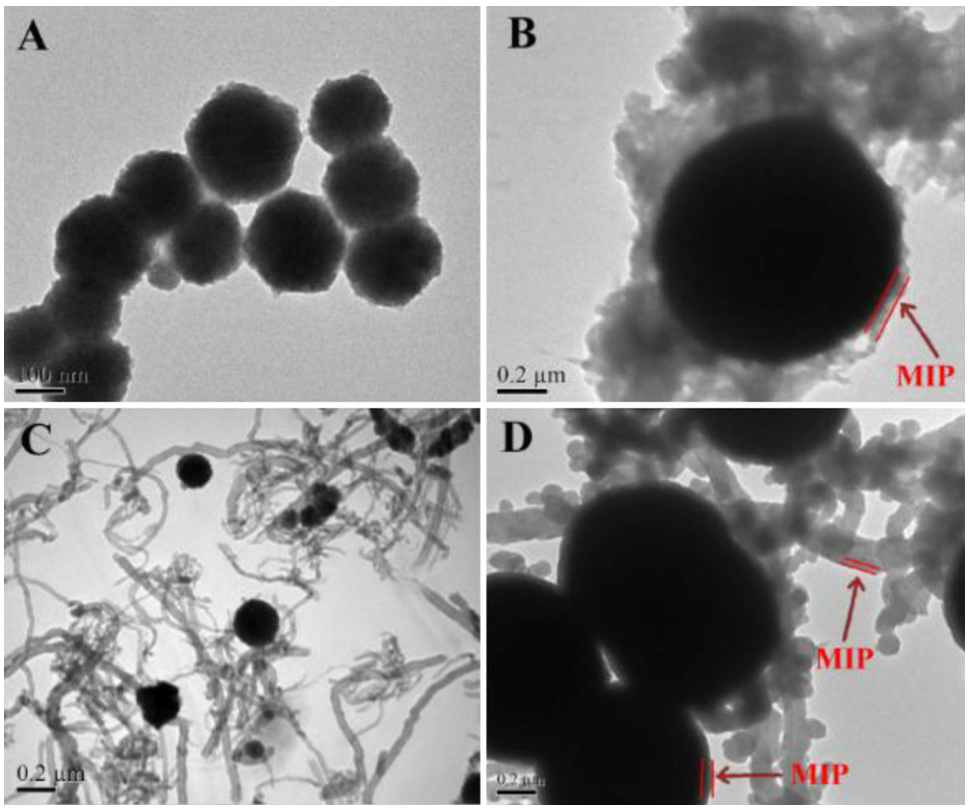

Fig. 2. TEM images of MNP (A), MNPs@MIP (B), MCNTs (C) and MCNTs@MIP (D).

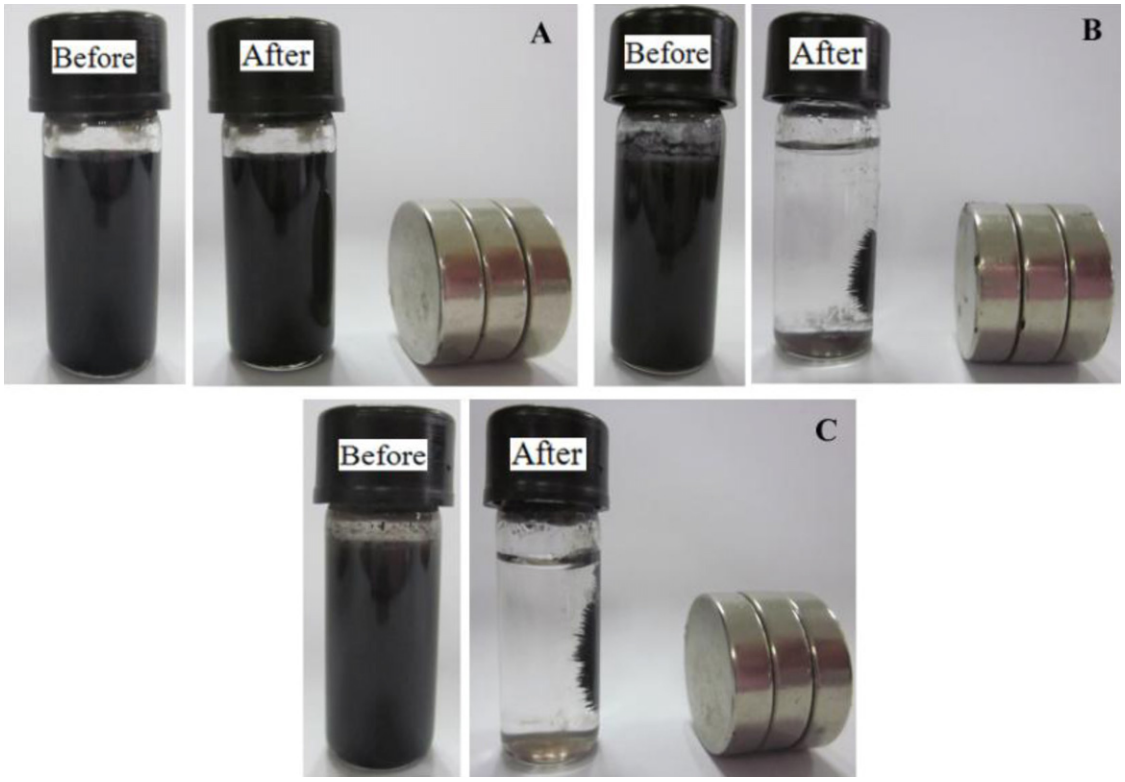

Fig. 3. Photographs of c-CNTs (A), MNPs@MIP (B) and MCNTs@MIP (C) before and after magnetic separation.

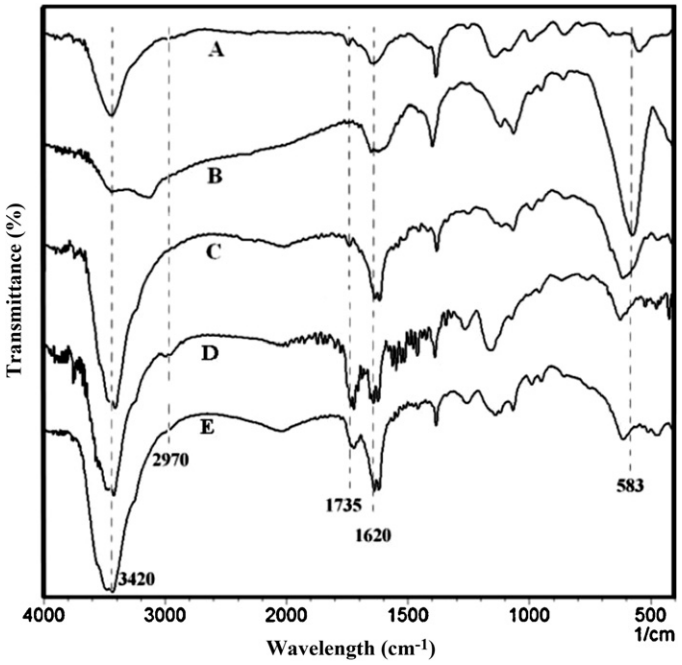

Fig. 4. FT-IR spectrum of c-CNTs (A), MNPs (B), MCNTs (C), MNPs@MIP (D) and MCNTs@MIP (E).

and E indicated that molecular imprinted polymer was successfully coated on the surface of MNPs and MCNTs, respectively.

3.3. Binding characteristics of imprinted materials

Fig. 5 presents the adsorption kinetics of GTFX solution onto MCNTs@MIP and MNPs@MIP. The adsorption capacity was increased with time and MCNTs@MIP exhibited a high adsorption rate. In the first 20 min, the adsorption rate was increased rapidly and reached equilibrium after 60 min. Such a time profile indicated an initial rapid increase in the adsorption capacity and later a slower increase to reach the adsorption equilibrium. For imprinted materials of non-thin films, it takes generally 12–24 h to reach adsorption equilibrium. However, imprinted materials of thin films only need 30–200 min to reach adsorption equilibrium for different templates [50]. Therefore, in our case, GTFX reached the surface imprinting cavities of MCNTs@MIP and MNPs@MIP easily and took less time to reach adsorption saturation, implying that the nanosized, surface

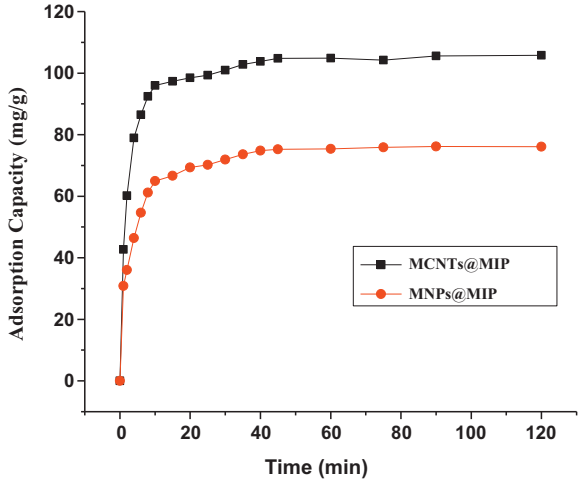

Fig. 5. Curves of adsorption kinetics of MCNTs@MIP and MNPs@MIP.

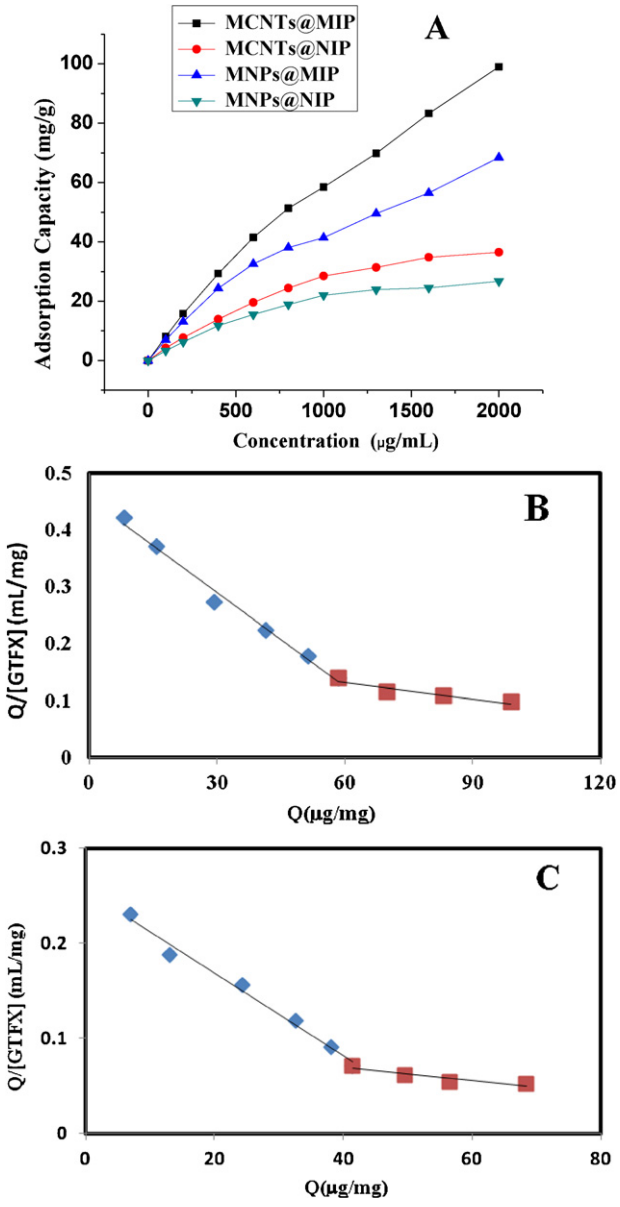

Fig. 6. Curves of adsorption isotherm of GTFX onto MCNTs@MIP, MCNTs@NIP, MNPs@MIP and MNPs@NIP (A); Scatchard plot to estimate the binding nature of MCNTs@MIP (B) and MNPs@MIP (C).

imprinting and uniform structures of MCNTs@MIP and MNPs@MIP allowed efficient mass transport, thus overcoming some drawbacks of traditionally packed imprinted materials.

The binding isotherms plotted in Fig. 6A indicated that the amount of GTFX bound to the MCNTs@MIP, MCNTs@NIP, MNPs@MIP and MNPs@NIP at binding equilibrium increased with the increasing of initial concentration of GTFX. The amount of GTFX bound to the MCNTs@MIP and MNPs@MIP was higher than that of MCNTs@NIP and MNPs@NIP, respectively. Scatchard analysis was also used for evaluation of the adsorption of MIP and NIP according to the equation:

$$\frac{Q}{[\mathrm{GTFX}]} = \frac{Q_{\max}}{K_D} - \frac{Q}{K_D} \quad (2)$$

where Q is the amount of GTFX bound to the materials at equilibrium; [GTFX] is the free GTFX concentration at equilibrium; K_D is the dissociation constant and Q_{max} is the apparent maximum binding amount. The values of K_D and the Q_{max} can

Table 1
Imprinting factors (α) and selectivity factors (β) of MIP and NIP.

Drug	Q (MCNTs@MIP) (mg/g)	Q (MCNTs@NIP) (mg/g)	α	β	Q (MNPs@MIP) (mg/g)	Q (MNPs@NIP) (mg/g)	α	β
GTFX	27.2	10.1	2.69		21.3	9.8	2.17	
CPFX	11.1	8.3	1.34	2.01	10.3	7.1	1.45	1.50
PZFX	7.1	7.3	0.97	2.77	6.5	6.7	0.97	2.23
AMX	3.7	3.9	0.94	2.86	3.2	3.4	0.94	2.31

be calculated from the slope and intercept of the linear line plotted in Q/[GTFX] versus Q. As shown in Fig. 6B and C, the binding sites of the plot were favorably linearized into two segments. It is suggested that there are probably higher affinity sites and lower affinity sites with MIPs. According to Eq. (2), the K_D and Q_{max} of MCNTs@MIP were calculated to be 181.8 μg/mL (0.484 μmol/mL) and 82.6 μg/mg (0.230 μmol/mg) for higher affinity site and 999.9 μg/mL (2.66 μmol/mL) and 192.7 μg/mg (0.513 μmol/mg) for lower affinity site. The K_D and Q_{max} of MNPs@MIP were calculated to be 232.6 μg/mL (0.620 μmol/mL) and 59.4 μg/mg (0.158 μmol/mg) for higher affinity site and 1428.6 μg/mL (3.81 μmol/mL) and 138.6 μg/mg (0.369 μmol/mg) for lower affinity site.

3.4. Adsorption selectivity

Selective recognition toward the template molecule, which depends on the imprinted cavities in complement to the size, shape, and functionality of the template molecule, is an important property for a novel imprinted material. Herein, the selectivity of the MCNTs@MIP, MCNTs@NIP, MNPs@MIP and MNPs@NIP toward the template and other quinolones was tested. PZFX was selected as referent to investigate the selectivity of the imprinted polymers. The imprinting factor (α) and selectivity factor (β) were used to evaluate the specific recognition property of the imprinted materials [51]. The imprinting factor is defined as follows:

$$\alpha = \frac{Q_A}{Q_B} \quad (3)$$

where Q_A and Q_B are the capacities of MIP and NIP to adsorb the template or referent. The selectivity factor is defined as follows:

$$\beta = \frac{\alpha_1}{\alpha_2} \quad (4)$$

where α_1 is the imprinting factor with respect to the template and α_2 is the imprinting factor with respect to referent.

As shown in Fig. S3, the capacity of MIP to adsorb GTFX was greater than their capacity to adsorb CPFX, PZFX and AMX. Additionally, the imprinting factors (α) of MCNTs@MIP and MNPs@MIP for the template were 2.69 and 2.17, respectively, which is bigger than those of referent. The selectivity factors (β) of referent are listed in Table 1, indicating that the adsorptions of referent by MCNTs@MIP and MNPs@MIP were lower.

3.5. Optimization of SPE procedure

In order to evaluate the applicability of MCNTs@MIP for extraction and determination of GTFX in serum samples, the parameters affecting the performance of the extraction, such as sample pH, MCNTs@MIP amount, adsorption time, desorption time and elute solvent, were investigated. The extraction conditions were optimized by analyzing spiked GTFX in serum samples (200 μg/mL). When one parameter was changed, the other parameters were fixed at their optimized values.

(a) *Sample pH*. pH value is essential not only for achieving high capacity, but also for bringing forward the selectivity of MCNTs@MIP. It has been known that the experimental pK_a values of gatifloxacin are 6.0 (pK_{a1}) and 9.2 (pK_{a2}). The pK_{a1} refers to the COOH-group and pK_{a2} refers to the $N_{4'}$ of the piperazine ring. At its isoelectric point at pH 7.6, most of the gatifloxacin molecules are zwitter-ions (net charge 0). The effect of pH was evaluated by preparing a Tris–HCl buffer. A pH range of 5.6–9.2 was studied. As shown in Fig. 7A, the best recoveries of GTFX were obtained at pH 7.4. It might be due to the physical–chemical properties of MCNTs@MIP and GTFX. To the best of our knowledge, there are multiple adsorption mechanisms such as imprinted cavities, π–π conjugate bonding and hydrophobic interactions present simultaneously and improved the adsorption ability of MCNTs@MIP. The results implied that π–π conjugate bonding and hydrophobic interactions between GTFX and MCNTs@MIP also played a key role in the adsorption.

(b) *MIP amount*. Different amounts of MIP ranging from 10 to 60 mg were applied to extract the GTFX from 5 mL serum samples (Fig. 7B). The results indicated that 50 mg MIP was enough, and satisfactory recoveries of GTFX for MCNTs@MIP (85.5%) were obtained. Further increasing the amount of MCNTs@MIP gave no improvement for recoveries of GTFX.

(c) *Adsorption time*. The effect of the extraction time from 10 to 70 min on the recoveries of GTFX was investigated (Fig. 7C). An increase in recovery was observed for GTFX with increasing contact time up to 60 min. Further increase in contact time does not result in significant increment in recovery but leads to a plateau. Therefore, in this work, the extraction time of 60 min was chosen for obtaining the complete extraction.

(d) *Desorption time*. GTFX recoveries were determined as a function of desorption time over the range from 10 to 80 min. As shown in Fig. 7D, a plateau is reached when desorption time is longer than 70 min.

(e) *Elute solvent*. In order to obtain the highest recoveries of GTFX, a series of elution solutions, acetone, methanol, acidified methanol were used to optimize the elution condition (Fig. 7E). Poor recoveries were found by using acetone and methanol. The best recoveries were obtained using 5 mL mixture of methanol/acetic acid (6:4, v/v) as eluting solution.

3.6. Application of imprinted materials in solid phase extraction of GTFX from serum samples

3.6.1. Analytical performances

After optimization of the extraction conditions, such as sample pH, MCNTs@MIP amount, adsorption time, desorption time and elute solvent, the linearity was evaluated with different concentrations of GTFX mixed standard solutions (0.006–500.00 μg/mL). The linear range of the MCNTs@MIP beads extraction coupled with HPLC method was established to be 0.80–450.00 μg/mL. The correlation coefficient of the calibration graphs is 0.9969. The LOD and LOQ were obtained from the diluted samples and the signal-to-noise ratio (S/N). According to the experimental results the LOD and LOQ of GTFX were 0.006 μg/mL (S/N = 3) and 0.015 μg/mL (S/N = 10), respectively. The enrichment factor is 10. The precision of the method was investigated with 20.00 μg/mL mixed standard solution of GTFX, and the relative standard deviations (RSDs) varied from 3.3 to 4.9% (n = 6).

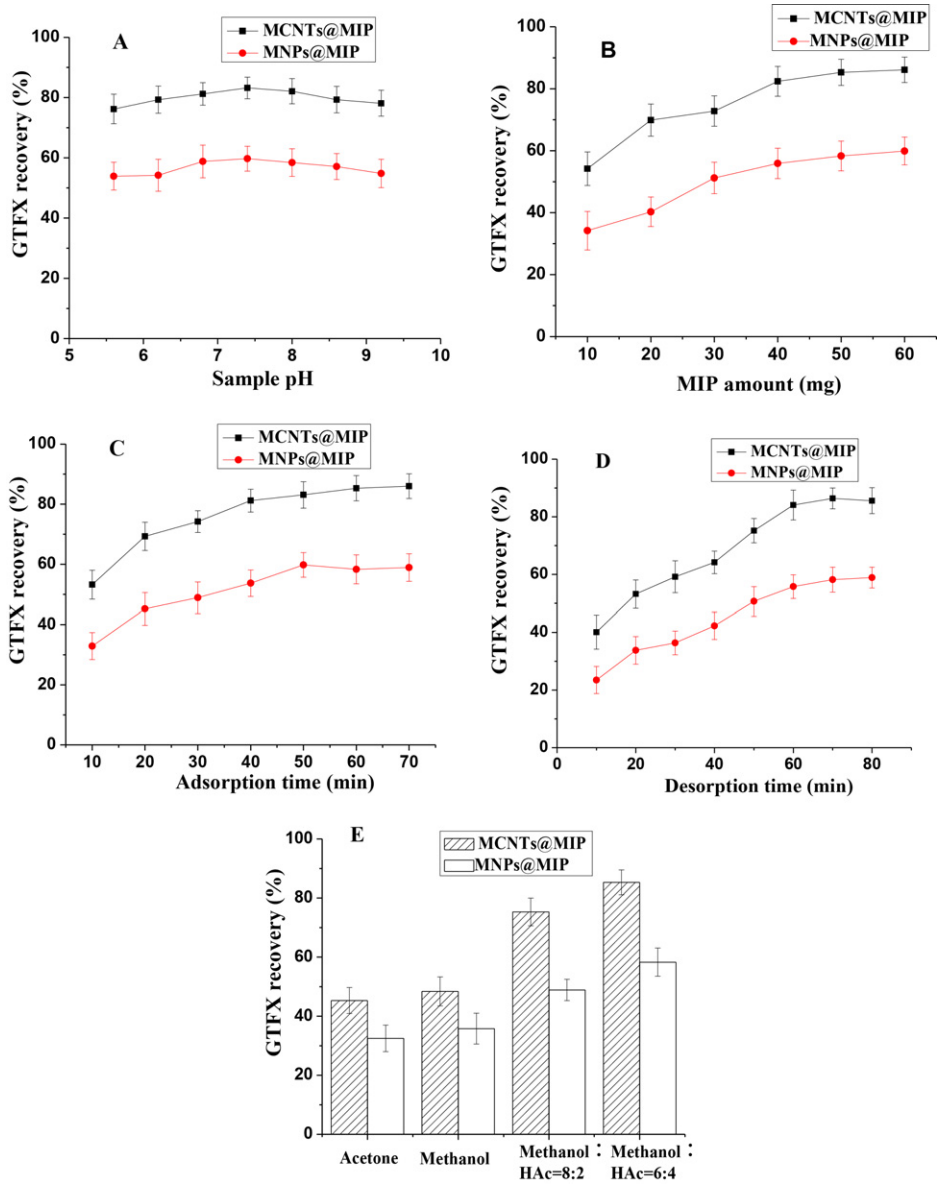

Fig. 7. The effects of sample pH (A), adsorption time (B), desorption time (C), MIP amount (D) and elute solvent (E) on the recoveries of GTFX ($n = 3$).

3.6.2. Serum sample analysis

As we known, prepared MIP which can be used in aqueous solutions is more challenging than that of in organic solvents [52–55]. In this paper, MCNTs@MIP and MNPs@MIP are both water-compatible and their application of selective adsorption of GTFX from aqueous solution or serum samples was investigated. As shown in Fig. 8, MCNTs@MIP demonstrated selective recognition toward the template molecule (GTFX), and the adsorption of referent (PZFX) was low. Moreover, due to the hydrophilic surface and selective recognition imprinted cavities of MCNTs@MIP, the adsorption of protein was low, so the recoveries of GTFX had no significant difference between in aqueous solution and serum samples. These results revealed that MCNTs@MIP could be directly used for selective adsorption and determination of GTFX in serum samples.

To evaluate the accuracy and application of the developed method, the aqueous solution and serum samples spiked with three levels of GTFX (2, 20 and 200 μg/mL) were analyzed. At each concentration, six measurements were performed. Applied MCNTs@MIP as a sorbent, the recoveries of GTFX in serum samples ranged from 79.1 ± 4.8% to 85.3 ± 4.2%, which were higher than that

Table 2
Recoveries of GTFX for spiked samples ($n = 6$).

Materials	Samples	2 μg/mL		20 μg/mL		200 μg/mL	
		Recovery (%)	RSD (%)	Recovery (%)	RSD (%)	Recovery (%)	RSD (%)
MCNTs@MIP	Aqueous solution	81.2	4.2	84.9	3.5	88.6	3.4
	Serum samples	79.1	4.8	81.8	4.3	85.3	4.2
MNPs@MIP	Aqueous solution	62.7	4.6	63.4	4.5	65.4	4.2
	Serum samples	55.6	5.4	56.3	4.9	58.3	4.8

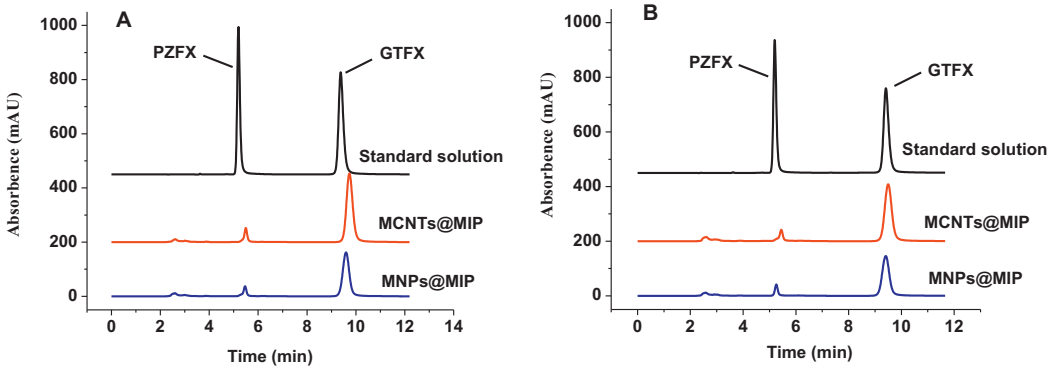

Fig. 8. Chromatograms of aqueous solution (A) and real serum samples (B) spiked with GTFX and PZFX at the concentration of 200 μg/mL. The black, red and blue lines represent the standard solution, solution recovered by MCNTs@MIP and MNPs@MIP, respectively. (For interpretation of the references to color in this figure legend, the reader is referred to the web version of the article.)

Table 3
Determination of gatifloxacin with different methods.

Method	Linear range (μg/mL)	LOD (ng/mL)	Recovery (%)	RSD (%)	Reference
LC/ESI-MS/MS	0.01–1	0.5	94.93–98.89	4.27	[56]
CPE-fluorimetry	0.0001–0.25	0.06	95.58–98.80	2.01	[5]
HPLC	–	30	102.0	2.3	[12]
MSPE-HPLC	0.80–450.00	6	79.1–85.3	4.2	This method

of MNPs@MIP (Table 2). The results indicated that the proposed method based on MCNTs@MIP was applicable for the extraction and determination of GTFX in serum samples. This method was comparable with LC/ESI-MS/MS [56], CPE-fluorimetry [5] and HPLC [12]. The results are listed in Table 3. To test the regeneration of MCNTs@MIP, five adsorption/desorption (regeneration) cycles were conducted with GTFX. The characteristics of the MCNTs@MIP are stable, which could be used for five cycles with lost of less than 7.8% of its recovery on average.

4. Conclusions

Attachment of Fe_3O_4 nanoparticles to carbon nanotubes was achieved by a simple solvothermal process. Then we developed an efficient method for synthesis of molecularly imprinted polymers using magnetic carbon nanotubes as support. The prepared MCNTs@MIP exhibited excellent specific recognition toward GTFX. Besides, they combined the magnetic properties of Fe_3O_4 nanoparticles with the outstanding mechanical properties and high surface area of CNTs. It could be easily separated from the suspension by an external magnetic field, leading to a fast and selective extraction of GTFX from serum samples. After MCNTs@MIP were reused and regenerated five times, the fifth recovery of GTFX was still excellent. We believe this novel surface imprinted polymers with magnetic carbon nanotubes as supports can be one of the most promising candidates for fast and selective extraction of therapeutic agents from biological fluids.

Acknowledgments

This work was supported by Graduate Students Innovative Projects of Jiangsu Province (No. CXZZ11_0812), Guizhou Provincial Natural Science Foundation of China (Grant No. J20122288), Zhejiang Provincial Natural Science Foundation of China (Grant No. Y4110235) and the Fundamental Research Funds for the Central Universities (Program No. JKY2011008).

Appendix A. Supplementary data

Supplementary data associated with this article can be found, in the online version, at http://dx.doi.org/10.1016/j.chroma.2012.12.011.

References

[1] L. Tasso, T.D. Costa, J. Pharm. Biomed. Anal. 44 (2007) 205.
[2] Y.F. Shi, H.L. Lv, X.F. Lu, Y.X. Huang, Y. Zhang, W. Xue, J. Mater. Chem. 22 (2012) 3889.
[3] C.-C. Li, A. Chauhan, Ind. Eng. Chem. Res. 45 (2006) 3718.
[4] A.S. Amin, A.A.E.-F. Gouda, R. El-Sheikh, F. Zahran, Spectrochim. Acta A 67 (2007) 1306.
[5] H. Wu, G.-y. Zhao, L.-m. Du, Spectrochim. Acta A 75 (2010) 1624.
[6] N.T.A. Ghani, M.A. El-Ries, M.A. El-Shall, Anal. Sci. 23 (2007) 1053.
[7] T.M. Reddy, K. Balaji, S.J. Reddy, J. Anal. Chem. 62 (2007) 168.
[8] L. Wang, P. Yang, Y. Li, H. Chen, M. Li, F. Luo, Talanta 72 (2007) 1066.
[9] B.R. Overholser, M.B. Kays, K.M. Sowinski, J. Chromatogr. B 798 (2003) 167.
[10] H.A. Nguyen, J. Grellet, B.B. Ba, C. Quentin, M.C. Saux, J. Chromatogr. B 810 (2004) 77.
[11] S. Al-Dgither, S.N. Alvi, M.A. Hammami, J. Pharm. Biomed. Anal. 41 (2006) 251.
[12] K. Borner, H. Hartwig, H. Lode, Chromatographia 52 (2000) S105.
[13] Y. Zhang, Y.W. Li, Y.L. Hu, G.K. Li, Y.Q. Chen, J. Chromatogr. A 1217 (2010) 7337.
[14] Z. Zhang, X. Yang, X. Chen, M. Zhang, L. Luo, M. Peng, S. Yao, Anal. Bioanal. Chem. 401 (2011) 2855.
[15] H.B. Zhang, Z.H. Zhang, Y.F. Hu, X.A. Yang, S.S. Yao, J. Agric. Food Chem. 59 (2011) 1063.
[16] F. Puoci, F. Iemma, G. Cirillo, M. Curcio, O.I. Parisi, U.G. Spizzirri, N. Picci, Eur. Polym. J. 45 (2009) 1634.
[17] H.J. Chen, Z.H. Zhang, L.J. Luo, S.Z. Yao, Sens. Actuators B: Chem. 163 (2012) 76.
[18] B. Rezaei, N. Majidi, A.A. Ensafi, H. Karimi-Maleh, Anal. Methods 3 (2011) 2510.
[19] S. Piperno, B. Tse Sum Bui, K. Haupt, L.A. Gheber, Langmuir 27 (2011) 1547.
[20] P. Qu, J. Lei, R. Ouyang, H. Ju, Anal. Chem. 81 (2009) 9651.
[21] Z. Zhang, H. Zhang, Y. Hu, S. Yao, Anal. Chim. Acta 661 (2010) 173.
[22] T. Akiyama, T. Hishiya, H. Asanuma, M. Komiyama, J. Incl. Phenom. Macrocyclic Chem. 41 (2001) 149.
[23] H. Zhang, P. Dramou, H. He, S. Tan, C. Pham-Huy, H. Pan, J. Chromatogr. Sci. 50 (2012) 499.
[24] X.W. Kan, Y. Zhao, Z.R. Geng, Z.L. Wang, J.J. Zhu, J. Phys. Chem. C 112 (2008) 4849.
[25] W. Luo, L. Zhu, C. Yu, H. Tang, H. Yu, X. Li, X. Zhang, Anal. Chim. Acta 618 (2008) 147.
[26] R. Gao, J. Zhang, X. He, L. Chen, Y. Zhang, Anal. Bioanal. Chem. 398 (2010) 451.
[27] X. Shen, L. Zhu, C. Huang, H. Tang, Z. Yu, F. Deng, J. Mater. Chem. 19 (2009) 4843.
[28] P. Qu, J. Lei, L. Zhang, R. Ouyang, H. Ju, J. Chromatogr. A 1217 (2010) 6115.
[29] Y. Hu, R. Liu, Y. Zhang, G. Li, Talanta 79 (2009) 576.

[30] R. Gao, X. Kong, X. Wang, X. He, L. Chen, Y. Zhang, J. Mater. Chem. 21 (2011) 17863.
[31] X. Kong, R. Gao, X. He, L. Chen, Y. Zhang, J. Chromatogr. A 1245 (2012) 8.
[32] M.A. Correa-Duarte, M. Grzelczak, V. Salgueiriño-Maceira, M. Giersig, L.M. Liz-Marzán, M. Farle, K. Sierazdki, R. Diaz, J. Phys. Chem. B 109 (2005) 19060.
[33] V. Georgakilas, V. Tzitzios, D. Gournis, D. Petridis, Chem. Mater. 17 (2005) 1613.
[34] C. Gao, W. Li, H. Morimoto, Y. Nagaoka, T. Maekawa, J. Phys. Chem. B 110 (2006) 7213.
[35] B. Jia, L. Gao, J. Sun, Carbon 45 (2007) 1476.
[36] D. Xiao, P. Dramou, H. He, L.A. Pham-Huy, H. Li, Y. Yao, C. Pham-Huy, J. Nanopart. Res. 14 (2012) 984.
[37] X. Liu, X. Wang, F. Tan, H. Zhao, X. Quan, J. Chen, L. Li, Anal. Chim. Acta 727 (2012) 26.
[38] M.-M. Zheng, R. Gong, X. Zhao, Y.-Q. Feng, J. Chromatogr. A 1217 (2010) 2075.
[39] H. Yan, F. Qiao, K.H. Row, Anal. Chem. 79 (2007) 8242.
[40] L. Chen, T. Wang, J. Tong, TrAC-Trends Anal. Chem. 30 (2011) 1095.
[41] K. Aguilar-Arteaga, J.A. Rodriguez, E. Barrado, Anal. Chim. Acta 674 (2010) 157.
[42] J.M. Pan, H. Yao, L.C. Xu, H.X. Ou, P.W. Huo, X.X. Li, Y.S. Yan, J. Phys. Chem. C 115 (2011) 5440.
[43] S.-W. Cao, Y.-J. Zhu, J. Chang, New J. Chem. 32 (2008) 1526.
[44] W. Shen, X. Chen, Y. Shi, M. Shi, H. Chen, Mater. Chem. Phys. 132 (2012) 987.
[45] C.-L. Lin, C.-F. Lee, W.-Y. Chiu, J. Colloid Interface Sci. 291 (2005) 411.
[46] S. Xuan, Y.-X.J. Wang, J.C. Yu, K. Cham-Fai Leung, Chem. Mater. 21 (2009) 5079.
[47] A. Rachkov, N. Minoura, J. Chromatogr. A 889 (2000) 111.
[48] M. Zhang, J. Huang, P. Yu, X. Chen, Talanta 81 (2010) 162.
[49] J. Ou, X. Li, S. Feng, J. Dong, X. Dong, L. Kong, M. Ye, H. Zou, Anal. Chem. 79 (2006) 639.
[50] R. Gao, X. Kong, F. Su, X. He, L. Chen, Y. Zhang, J. Chromatogr. A 1217 (2010) 8095.
[51] W. Zhang, L. Qin, X.-W. He, W.-Y. Li, Y.-K. Zhang, J. Chromatogr. A 1216 (2009) 4560.
[52] B. Dirion, Z. Cobb, E. Schillinger, L.I. Andersson, B. Sellergren, J. Am. Chem. Soc. 125 (2003) 15101.
[53] G. Pan, Y. Zhang, Y. Ma, C. Li, H. Zhang, Angew. Chem. Int. Ed. 50 (2011) 11731.
[54] G. Pan, Y. Zhang, X. Guo, C. Li, H. Zhang, Biosens. Bioelectron. 26 (2010) 976.
[55] R. Gao, X. Su, X. He, L. Chen, Y. Zhang, Talanta 83 (2011) 757.
[56] K. Vishwanathan, M.G. Bartlett, J.T. Stewart, Rapid Commun. Mass Spectrom. 15 (2001) 915.